

Optimization of Integrated Multi-stage Complementary Energy Systems for Hydrogen Production, Storage and Utilization

Luoxian Huang^a, Jin Sun^{a,*}, Dominic C. Y. Foo^b, Xingye Zeng^a, Li Wang^a, Shaolin Hu^c, Yuan Lu^d

^aSchool of Chemical Engineering, Guangdong University of Petrochemical Technology, Maoming 525000, China

^bDepartment of Chemical & Environmental Engineering, University of Nottingham Malaysia, Broga Road, 43500 Semenyih, Selangor, Malaysia

^cSchool of Automation, Guangdong University of Petrochemical Technology, Maoming 525000, China

^dMaoming Ruipai Petrochemical Engineering Co., Ltd., Maoming 525000, China
[sunjin@gdupt.edu.cn](mailto:sunjing@gdupt.edu.cn)

Under the dual-carbon targets, renewable energy integration has been extensively studied; however, the volatility of wind and photovoltaic power continues to hinder stable and cost-efficient operation. Most existing works focus on single energy carriers or partial optimization, leaving gaps in the holistic coordination of electricity, heat, gas, and hydrogen flows, particularly under carbon trading and demand response mechanisms. To address this, we propose an integrated optimization model for a hydrogen-centered multi-energy complementary system that incorporates wind and photovoltaic power, energy storage batteries, electrolyzers, fuel cells, hydrogen storage, and synthetic natural gas units. The model employs a mixed-integer quadratic programming (MIQP) approach to enhance system flexibility and minimize total operating costs. Simulation results verify the effectiveness of the proposed model in improving renewable energy utilization, reducing carbon emissions, and promoting low-carbon transition in industrial parks. This study provides a practical framework for advancing multi-energy system integration under the hydrogen economy paradigm.

1. Introduction

Achieving dual-carbon goals is driving the rapid shift toward clean energy, with wind and solar power emerging as key resources. Yet their inherent intermittency continues to hinder stable and cost-effective operation, while fossil fuels remain dominant and contribute to emissions and energy security concerns. Hydrogen has been widely recognized as a zero-carbon alternative, with applications ranging from fuel cells to energy storage. Previous studies have explored hydrogen in specific contexts, such as PEMFC-based CHP modelling with Artificial Neural Networks (Asensio et al., 2017), hydrogen transport via compressed gas trucks (Lahnaoui et al., 2018), and off-grid solar charging stations incorporating hydrogen storage (Mehrerjedi, 2019). These works demonstrate hydrogen's potential but remain fragmented, focusing on isolated technologies or subsystems. This study advances the field by proposing an integrated optimization framework for a hydrogen-centered multi-energy complementary system. Unlike existing approaches, our model holistically coordinates electricity, heat, gas, and hydrogen flows while explicitly embedding carbon trading and price-based demand response. A mixed-integer quadratic programming (MIQP) formulation is employed to capture both operational flexibility and cost efficiency. Simulation results confirm that the model not only improves renewable utilization and reduces carbon emissions but also offers a scalable pathway for industrial parks to achieve low-carbon transformation under the hydrogen economy paradigm.

2. Integrated Hydrogen Energy System Framework and mathematic model

This study proposes an optimization model for a hydrogen-centered, multi-level energy complementary system that considers electricity, hydrogen, natural gas, and heat demands. The model integrates energy conversion technologies to enhance operational flexibility and leverages carbon trading and demand response mechanisms

to coordinate energy supply and demand, achieving economically efficient system operation. A mixed-integer quadratic programming (MIQP) approach is employed to model and optimize the system, and case studies are conducted to validate model feasibility and performance. This research aims to provide theoretical guidance and practical references for the efficient operation and sustainable development of multi-energy systems under the hydrogen economy paradigm.

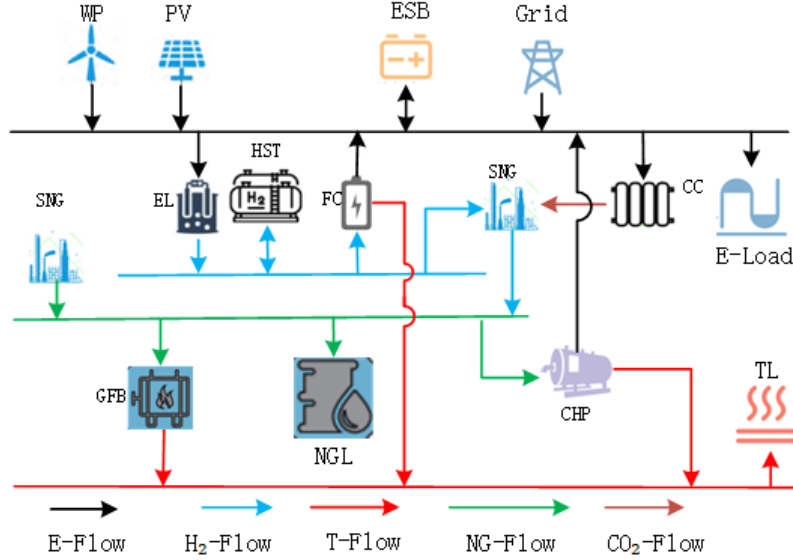


Figure 1: Integrated Multi-Level Energy Complementary System Framework for Hydrogen Production, Storage, and Utilization

In this study, a multi-energy complementary system is developed integrating various energy sources and conversion units. The system components and corresponding abbreviations used throughout the paper are as follows: Wind Power (WP), Photovoltaic (PV), Energy Storage Battery (ESB), External Power Grid (Grid), Hydrogen Storage Tank (HST), Fuel Cell (FC), Electrolyzer (EL), and Synthetic Natural Gas (SNG). The system also considers Electric Load (EL), Thermal Load (TL), and Natural Gas Load (NGL) as key demand-side factors. Energy flows are denoted by Electric Energy Flow (E-Flow), Hydrogen Energy Flow (H₂-Flow), Carbon Dioxide Flow (CO₂-Flow), Thermal Energy Flow (T-Flow), and Natural Gas Energy Flow (NG-Flow). Additionally, Chemical Conversion (CC) refers to processes such as converting captured carbon (CC) and hydrogen into synthetic fuels, including SNG. Combined Heat and Power Units (CHP) and Gas-fired Boilers (GFB) are also included to meet heating demands and enhance system flexibility.

3. Objective Function and constraints

3.1 Objective Function

The objective function of the integrated multi-level energy complementary system optimization model for hydrogen production, storage, and utilization constructed in this paper is to minimize the system operation cost. It mainly includes carbon emission cost, equipment operation and maintenance cost, and energy purchasing cost. The specific mathematical model is as follows:

$$F = F_{buy} + F_{om} + F_{co_2} \quad (1)$$

where F denotes the system operation cost; F_{buy} denotes the energy purchasing cost; F_{om} denotes the equipment operation and maintenance cost; F_{co_2} denotes the carbon emission cost.

(1) Energy Purchasing Cost

$$F_{buy} = \sum_{t=1}^T (f_e(t) + f_g(t)) \quad (2)$$

where $f_e(t)$ is the electricity purchasing cost at time t ; $f_g(t)$ is the gas purchasing cost at time t ; T is the dispatching period.

3.2 Equipment Operation and Maintenance Cost

$$F_{om} = \sum_{t=1}^T (f_{om,i}(t) \times P_i(t)) \quad (3)$$

where $f_{om,i}(t)$ is the operation and maintenance cost coefficient (in RMB/kW) of equipment i at time t ; $P_i(t)$ is the output power of equipment i at time t (kW/h); i represents wind power (w), photovoltaic (v), energy storage system (ess), electrolyzer (et), fuel cell (fc), hydrogen storage system (hss), hydrogen boiler (hb), and combined heat and power gas turbine (gt). The set is $\{w, v, ess, et, fc, hss, hb, gt\}$.

In the constructed integrated hydrogen production, storage, and utilization multi-level energy complementary system optimization model, the main sources of carbon emissions are the external power grid, the combined heat and power unit, and the CO₂ consumed in hydrogen synthetic natural gas processes. The specific mathematical model is:

$$F_{co_2} = \lambda (E_{IES,a} - E_{e,buy} - E_g) \quad (4)$$

$E_{IES,a}$ is the actual total carbon emission of the energy system constructed in this paper (t/y); $E_{e,buy}$ is the free carbon emission quota for electricity purchased from the upper-level power grid (t/y); E_g is the total free carbon emission quota for energy conversion of combined heat and power and gas boiler equipment (t/y); λ is the carbon trading price coefficient (RMB/t).

3.3 Constraints

The optimization model constructed in this paper for the integrated hydrogen production, storage, and utilization multi-level energy complementary system needs to consider equipment operation constraints, power grid system constraints, and planning constraints. The specific mathematical models are as follows:

3.3.1 System Constraints

The energy complementary system designed in this paper considers the electric power system, thermal energy system, and natural gas system. Since energy supply and demand need to be balanced in real-time, the following energy balance constraints must be satisfied:

(1) Electricity Balance Constraint

$$P_t^w + P_t^v + P_t^{buy} + P_t^{es,dis} + P_t^{GT} + P_t^{HFC} \geq P_t^{dr,load} + P_t^{es,cha} + P_t^{EL} + P_t^{CCS} \quad (5)$$

Where P_t^{buy} is the power purchased from the grid; $P_t^{es,dis}$ and $P_t^{es,cha}$ are the battery discharging and charging power; P_t^{GT} and P_t^{HFC} are the outputs of the gas turbine and fuel cell; P_t^{EL} and P_t^{CCS} are the power consumption of the electrolyzer and carbon capture unit; $P_t^{dr,load}$ is the user demand; and P_t^w and P_t^v are the wind and photovoltaic generation.

(2) Thermal Energy Balance Constraint

$$H_t^{HFC} + H_t^{GB} + H_t^{GT} \geq H_t^{load} \quad (6)$$

Where H_t^{HFC} is the heat output from the fuel cell, H_t^{GB} is the heat output from the gas boiler, H_t^{GT} is the heat output from the CHP system, and H_t^{load} is the user heat load demand at time t .

(3) Natural Gas Balance Constraint

$$G_t^{buy} + G_t^{MR} \geq G_t^{load} + G_t^{GB} + G_t^{GT} \quad (7)$$

Where G_t^{buy} is the natural gas purchased from the upper-level network, G_t^{MR} is the synthetic natural gas production, G_t^{load} is the user natural gas demand, G_t^{GB} is the gas consumption of the boiler, and G_t^{GT} is the gas consumption of the turbine at time t .

3.3.2 Operating Constraints of Equipment

In the integrated multi-level energy complementary system designed in this paper for hydrogen production, storage, and utilization, the following equipment is considered: electrolyzer, electrical energy storage device, hydrogen energy storage device, synthetic natural gas (SNG) equipment, fuel cell, carbon capture unit, gas-fired boiler, and gas turbine. The specific mathematical models are as follows:

(1) Electrolyzer Equipment

$$H_{2t}^{EL} = \eta_{EL} P_t^{EL} \quad (8)$$

$$0 \leq P_t^{EL} \leq P_{EL,max} \quad (9)$$

$$P_{t+1}^{EL} - P_t^{EL} \leq \eta_{pp} P_{EL,max} \quad (10)$$

$$P_t^{EL} - P_{t+1}^{EL} \leq \eta_{pp} P_{EL,max} \quad (11)$$

In the equations, H_{2t}^{EL} represents the hydrogen power generated by the electrolyzer at time t ; η_{EL} denotes the electricity-to-hydrogen energy conversion efficiency of the electrolyzer; $P_{EL,max}$ indicates the upper limit of the electrical power consumed by the electrolyzer; and η_{pp} represents the ramp rate coefficient. Eqs(8)–(11) describe, respectively, the energy conversion constraint from electricity to hydrogen in the electrolyzer, the upper and lower output limits of the electrolyzer, as well as the ramp-up and ramp-down constraints.

(2) Battery Energy Storage System (BESS)

$$SOC_t^e = (1 - \rho) SOC_{t-1}^e + P_t^{cha} \eta_{cha}^e - P_t^{dis} / \eta_{dis}^e \quad (12)$$

$$0 \leq P_t^{cha} \leq d_t^{e,cha} P_{cha,max} \quad (13)$$

$$0 \leq P_t^{dis} \leq d_t^{e,dis} P_{dis,max} \quad (14)$$

$$d_t^{e,dis} + d_t^{e,cha} \leq 1 \quad (15)$$

$$SOC_{min}^e \leq SOC_t^e \leq SOC_{max}^e \quad (16)$$

Eqs(12)–(16) represent the operational constraints of the battery energy storage system. Specifically, Eq(12) defines the state-of-charge update constraint, ensuring the energy balance across time steps. Eq(13) imposes the upper limit on charging power at time t , while Eq(14) specifies the upper limit on discharging power at time t . Eq(15) introduces the mutual exclusivity condition, which prevents the battery from charging and discharging simultaneously. Finally, Eq(16) enforces the upper and lower bounds on the total stored energy at time t . Meanwhile, in order to ensure that the energy storage system can continue to participate in the next scheduling cycle, the total stored energy of the battery energy storage system at the end of the current scheduling period must be equal to that at the initial time. The corresponding mathematical model is formulated as follows:

$$SOC_0^e = SOC_{24}^e \quad (17)$$

(3) Hydrogen Energy Storage System

$$SOC_{min}^{e,H_2} \leq SOC_t^{e,H_2} \leq SOC_{max}^{e,H_2} \quad SOC_t^{H_2} = (1 - \rho) SOC_{t-1}^{H_2} + H_{2t}^{cha} \eta_{cha}^{H_2} - H_{2t}^{dis} / \eta_{dis}^{H_2} \quad (18)$$

$$SOC_{min}^{e,H_2} \leq SOC_t^{e,H_2} \leq SOC_{max}^{e,H_2} \quad 0 \leq H_{2t}^{cha} \leq d_t^{H_2,cha} H_{2cha,max} \quad (19)$$

$$SOC_{\min}^e \leq SOC_t^e \leq SOC_{\max}^e \quad 0 \leq H_{2t}^{dis} \leq d_t^{H_2,dis} H_{2dis,max} \quad (20)$$

$$SOC_{\min}^e \leq SOC_t^e \leq SOC_{\max}^e \quad d_t^{H_2,dis} + d_t^{H_2,cha} \leq 1 \quad (21)$$

$$SOC_{\min}^e \leq SOC_t^e \leq SOC_{\max}^e \quad SOC_{\min}^{H_2} \leq SOC_t^{H_2} \leq SOC_{\max}^{H_2} \quad (22)$$

Eqs(18)–(22) define the hydrogen storage system constraints, including the state-of-charge update, charging and discharging power limits at time t , the mutual exclusivity of charging and releasing, and the bounds on stored hydrogen energy. Meanwhile, in order to ensure that the hydrogen storage system can continue to participate in the next scheduling period, the total amount of stored hydrogen energy at the end of the current cycle must be equal to that at the initial time. The corresponding mathematical model is given as follows:

$$SOC_0^{H_2} = SOC_{24}^{H_2} \quad (23)$$

4. Analysis of Operation Results

In Scenario 1, hydrogen production, storage, and utilization technologies are not considered, which basically serves as our baseline model for comparison and validation. Since wind and photovoltaic power exhibit reverse peak-shaving characteristics, the system operation in Scenario 1 heavily depends on purchasing natural gas to meet user heat and gas load demands. In Scenario 1, heat supply mainly relies on gas turbines and gas boilers., Hydrogen production, storage, and utilization into the model are introduced in Scenario 2. Figure 2 shows the electrical power output of various devices in the system under Scenario 2.

From Figure 2, during the periods 1:00–9:00 and 21:00–24:00, wind power output is relatively high while the system's electricity demand is low. At the same time, the electricity price for purchasing power from the upstream grid is low. Under these conditions, the system converts surplus electric energy into hydrogen energy through the electrolyzer, realizing the electric-to-hydrogen energy conversion and enhancing system operational flexibility. Between 11:00 and 16:00, when wind power output is low and the system's electricity demand is high, the conversion from electric energy to hydrogen energy is stopped, and all energy is used to supply the electrical load.

The carbon emission cost in Scenario 1 is 6,210.475 RMB. In Scenario 2, carbon capture equipment is introduced. During periods of energy surplus and low electric load (1:00–9:00 and 21:00–24:00), the system reduces CO₂ emissions through the use of carbon capture devices. This reduces the carbon emission cost from 6,210.475 RMB in Scenario 1 to 4,154.633 RMB in Scenario 2, achieving an effective reduction of 33.103 %.

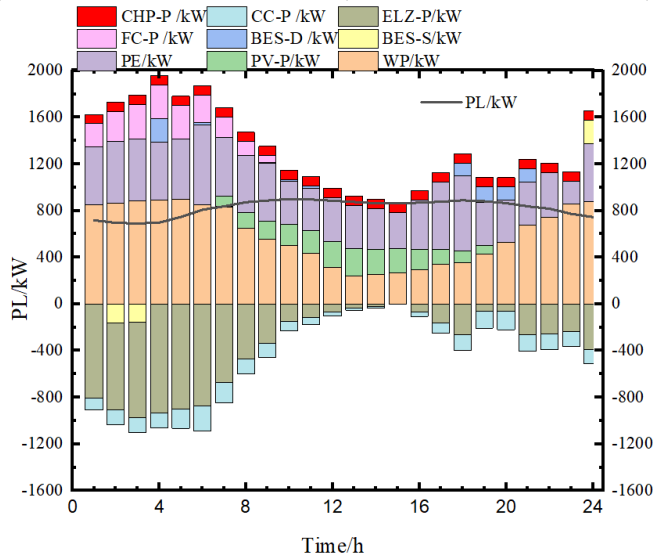


Figure 2: Electrical Power Output of System Devices in Scenario 2

Figure 3 shows the user's electricity load before and after participating in demand response. It can be seen that before participation, the user's electricity demand mainly concentrates between 10:00 and 19:00. Due to natural

conditions, the wind turbine output mainly occurs between 1:00–9:00 and 21:00–24:00, opposite to the user's energy demand peaks. This results in a counter-peak characteristic of wind power output.

Electricity market prices can guide price-sensitive users to adjust their energy usage times. For example, between 11:00–15:00 and 17:00–20:00, when wind power output is low and electricity prices are high, demand response encourages users to reduce electricity consumption. Conversely, between 1:00–8:00 and 21:00–24:00, when wind power output is high and electricity prices are relatively low, price signals encourage users to increase electricity consumption.

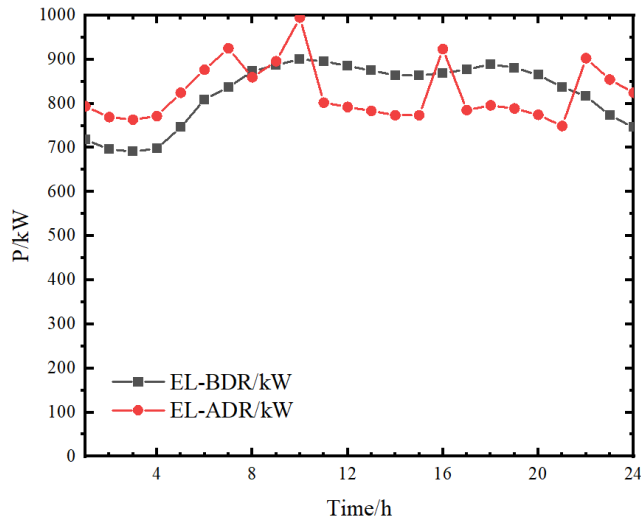


Figure 3: User Electricity Load Before and After Participating in Demand Response

The case study is extended by incorporating a recuperator to the base case ORC process, in order to improve its power generation efficiency. Specifically, a new heat exchanger (recuperator) is added so that the heat flow from the turbine outlet may be utilized to preheat the cold flow from the pump outlet (see simulation flowsheet

5. Conclusions

In this study, a multi-energy complementary system integrating hydrogen production, storage, and utilization is proposed to address the operational challenges of high renewable penetration under the dual-carbon background. The system incorporates key components such as wind and photovoltaic power generation, battery storage, electrolyzers, hydrogen storage tanks, fuel cells, and synthetic natural gas equipment. A coordinated optimization model is constructed with the goal of minimizing total operational cost, considering electricity, heat, gas, and hydrogen energy flows, as well as carbon emissions and demand response mechanisms. The model is formulated as a mixed-integer quadratic programming problem to accurately capture operational constraints and economic factors.

Acknowledgments

This research was funded by the Maoming City Science and Technology Plan Project (Project No.: 2025762), Guangdong Provincial Undergraduate Universities Higher Education Teaching Reform Project (710135181038) and Teaching Quality Project (710135181032).

References

- Asensio F.J., San Martín J.I., Zamora I., García-Villalobos J., 2017, Fuel cell-based CHP system modelling using Artificial Neural Networks aimed at developing techno-economic efficiency maximization control systems. *Energy*, 123, 585-593.
- Lahnaoui A., Wulf C., Heinrichs H., Dalmazzone D., 2018, Optimizing hydrogen transportation system for mobility by minimizing the cost of transportation via compressed gas truck in North Rhine-Westphalia. *Applied Energy*, 223, 317-328.
- Mehrjerdi H., 2019, Off-grid solar powered charging station for electric and hydrogen vehicles including fuel cell and hydrogen storage. *International Journal of Hydrogen Energy*, 44(23), 11574-11583.